Beam test of a small MICROMEGAS DHCAL prototype

C. Adloff, J. Blaha, M. Chefdeville[*]**, A. Dalmaz, C. Drancourt, A. Espargilière, R. Gaglione, Y. Karyotakis, J. Prast and G. Vouters**

Laboratoire d'Annecy-le-Vieux de Physique des Particules, Université de Savoie, CNRS/IN2P3, France
E-mail: `chefdevi@lapp.in2p3.fr`

ABSTRACT: A sampling hadronic calorimeter with gaps instrumented with thin MICROMEGAS chambers of small pad size and single bit readout is a candidate for an experiment at a future linear collider.

Several MICROMEGAS chambers with 1 cm^2 anode pads were fabricated using the Bulk technology. Some prototypes equipped with analog readout GASSIPLEX chips were developed for characterisation at the CERN/PS facility. A stack of four chambers and stainless steal absorber plates was used to assess the behaviour of MICROMEGAS in 2 GeV electron showers. Longitudinal and transverse shower profile are shown.

The Bulk fabrication process was adapted to laminate a mesh on anode PCBs with front-end chips connected on the backside. It is well suited for the construction of a 1 m^3 DHCAL MICROMEGAS prototype as large and thin chambers can be made. Such chambers with digital readout chips (HARDROC or DIRAC) were fabricated and tested in a beam. First results are presented.

KEYWORDS: ILC, DHCAL, MICROMEGAS, Shower profile, HARDROC, DIRAC.

---

[*]Corresponding author.

Contents

1. Introduction

1.1 Calorimetry at a future electron collider

Several important physics measurements that could be realized at a future electron linear collider (ILC or CLIC) would require a very good jet energy resolution (3 % at 100 GeV) [1]. The Particle Flow Approach (PFA) has been proposed to reach such a resolution. It consists in measuring the energy of the each particle contained in a jet with the tracker or with the calorimeters depending on its charge. While charged particle energy is measured with the tracker (which is more precise than the calorimeters), neutral particle energy is deduced from the energy deposit in the calorimeter from which the contribution of charged particles is subtracted. This calls for finely segmented calorimeters with single shower imaging capability.

1.2 Digital hadronic calorimetry

A digital hadronic calorimeter (DHCAL) would balance the cost of an increased number of readout channels (with a cell size of 1 cm^2, the number of channel would reach $3 \cdot 10^7$) by a simpler readout circuitry (1 bit information per channel). A DHCAL can be instrumented with scintillating or gaseous layers. In the latter case, GEMs [2, 3], RPCs [4] and MICROMEGAS [5, 6] are being considered. Some benefits of a MICROMEGAS DHCAL are a potentially high efficiency for MIPs, a hit multiplicity close to 1, low working voltages w.r.t. GEMs and RPCs (400–500 V), a thin sensitive layer (3 mm of Ar), a very good long-term irradiation behaviour and a high rate capability.

1.3 Scope of the study

We built several Bulk MICROMEGAS chambers with 1 cm^2 anode pads [10]. Some chambers are read out by GASSIPLEX chips [7] which measure the charge. They are used for detector characterisation in electron and hadron showers. Other chambers are equipped with DIRAC [9] or HARDROC [8] chips which provide a 3 or 2 bit information per channel. They are intended for constructing a 1 m^3 DHCAL prototype.

The behaviour of MICROMEGAS in electromagnetic showers has been studied at the PS facility at CERN. Because of the small number of chambers available, this study was carried out with one 12×32 cm^2 chamber with GASSIPLEX readout in front of which were placed a variable number of stainless steal absorber plates. Measurements of energy profile are presented in section 3. These are important to verify that MICROMEGAS performance is maintained in high track multiplicity showers. Finally, first tests in a beam of HARDROC and DIRAC based MICROMEGAS chambers are reported in section 4.

2. Experimental setup

2.1 Chamber geometry and readout electronics

The chambers consist of an anode PCB segmented into 1 cm^2 pads, a woven mesh maintained 128 μm above the PCB by insulating pillars [10], a 3 mm thick plastic frame which defines the drift region and a 2 mm thick grounded steel cover. The drift electrode is a copper foil glued on a kapton, itself glued on the cover surface. The gas is flushed in the chamber through two holes in the plastic frame. Measurements reported in this paper are performed in Ar/iC$_4$H$_{10}$ 95/5.

Four chambers with GASSIPLEX readout were built: three of 6×16 cm^2 and one of 12×32 cm^2 (called G$_1$, G$_2$, G$_3$ and G$_4$). The corresponding number of pads is equal to 96 and 384 respectively. GASSIPLEX is a 16 channel ASIC that amplifies and shapes the pad signals. Boards equipped with 6 chips are connected on the side of the chambers. The resulting signals are digitized by 10 bit ADCs placed in a crate.

One 8×8 cm^2 chamber read out by a DIRAC ASIC and three 8×32 cm^2 chambers read out by HARDROCs have been constructed (called D$_0$, H$_1$, H$_2$ and H$_3$). Pads of 1 cm^2 are first patterned on one side of a PCB. In order to reduce the chamber thickness, the ASICs are then connected on the backside. Finally, the MICROMEGAS is laminated onto the PCB. The total thickness of these

chambers with embedded electronics is smaller than 8 mm. This is already compatible with the ILC HCAL specification for gap size between absorbers.

2.2 Beam test setup

The beam test took place in June 2009 in the CERN/PS/T10 zone where electrons, positrons and hadrons with momenta up to 10 GeV/c are delivered. At 2 GeV/c, the ratio between electrons/positrons and hadrons is roughly 1:1 and the momentum spread of about 1 %.

The setup consists of a stack of four GASSIPLEX (G_1–G_4) and three HARDROC chambers (H_1–H_3) (Figure 1). The stack position is such that the beam impinges perpendicularly on the chambers. For triggering purposes, three 8×32 cm^2 scintillators (S_1, S_2 and S_3) are placed inside the stack parallel to the chamber planes. Two 2×4 cm^2 scintillators (S_4 and S_5) perpendicular to each other and parallel to the chamber planes are also available. They are placed in front of the stack. With an overlap area of 1 cm^2 they can be used to reduce the trigger angular acceptance.
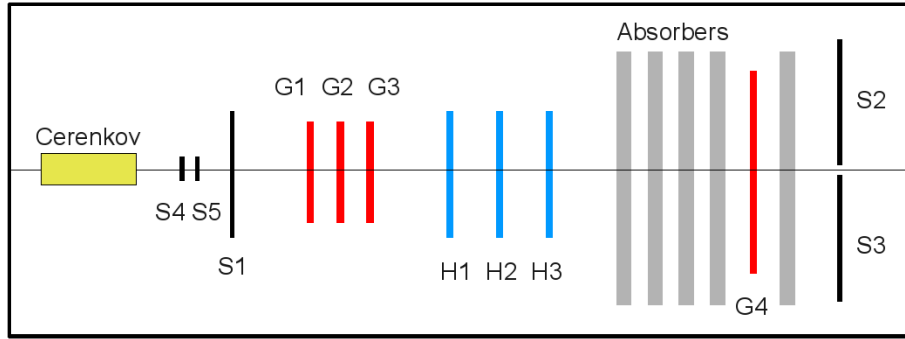
Figure 1. Beam test setup.

Shower profiles are measured with the chamber G_4 in front of which a variable number of absorbers are placed. Up to 12 steel plates each of 2 cm thick can be installed in front of G_4. The gap between each absorber is equal to 8 mm. One absorber is placed a few cm behind G_4 to allow backscattering of the shower particles to the chamber.

A Čerenkov counter installed in the T10 zone ahead of the stack is filled with CO_2 at 4 bars. The threshold velocity β_{th} is equal to 0.9983. At 2 GeV/c, protons and pions are too slow ($\beta = 0.8831$ and 0.9976) to produce Čerenkov light. Counter signals are hence used to discriminate between 2 GeV/c electrons/positrons and hadrons.

The chamber equipped with a DIRAC chip was tested in August 2008 in the SPS/H2 beam line. No trigger device was used and the test setup consisted mainly of the chamber itself.

3. Beam test of GASSIPLEX readout chambers

3.1 Energy deposit measurement

The number of ADC counts N (after pedestal subtraction) measured on a given channel relates to the energy deposited in the gas ε above the corresponding pad. Neglecting the transverse diffusion of the primary electrons and assuming that the amplified signal does not saturate the electronics, N relates to ε according to:

$$N = \frac{q_e G S}{W} \varepsilon \qquad (3.1)$$

with G the gas gain, S the conversion factor of the electronics (in ADC counts per unit of charge), W the mean energy per ion pair and q_e the electron charge. The total energy ξ deposited in the chamber is the sum of the energy measured on all pads with signals larger than a hit threshold of 15 ADC counts (3 fC). Taking the channel to channel variations of gas gain and conversion factor, the sum can be written as:

$$\xi = \sum_i \varepsilon_i = \frac{W}{q_e} \sum_i \frac{N_i}{G_i S_i} \qquad (3.2)$$

In the future, these measurements will be compared to predictions from a GEANT4 simulation. In the latter case, the drift gap is uniform across the detector area. This is not the case in practice and therefore the measured energy should be corrected for these variations. This could be done by weighting N_i with the ratio $d_i/\overline{d}$ with d_i the gap thickness above the channel pad i and $\overline{d} = 3$ mm. The values of d_i could not be measured but can be combined with G_i and S_i in the factor w_i:

$$\xi = \frac{W}{q_e} \frac{1}{\overline{G}\,\overline{S}} \sum_i \frac{\overline{G}\,\overline{S}}{\overline{d}} \frac{d_i}{G_i S_i} N_i = \frac{W}{q_e} \frac{1}{\overline{G}\,\overline{S}} \sum_i w_i N_i \qquad (3.3)$$

with $\overline{G}$ and $\overline{S}$ the gas gain and conversion factor averaged over all channels. $\overline{S}$ is determined from a calibration of all channels. The gas gain could only be measured on a single pad (by means of an ^{55}Fe source) and $\overline{G}$ is taken as the gain on that pad. This introduces an error on the measured energy that we estimate to lie below 5 % from the Bulk gap thickness specifications and the gain sensitivity to gap variations . The determination of the weight w_i of each channel is called the inter-calibration and is explained in the next section. In addition, the gas gain is a function of pressure and temperature and may change with time. As will be shown in section 3.3, such gain variations during the beam test are not negligible and corrections for these will be applied.

3.2 Channel inter-calibration

The channel weights are determined by scanning the area of chamber G_4 with the beam. The acquisition is triggered by the time coincidence of the S_1 and S_2 (or S_1 and S_3) scintillator signals. Neglecting variations of the incident angle of the tracks, the weights are given by the most probable value w_i of the ADC count distribution on each channel:

$$w_i = \frac{m_i}{\overline{m}} \qquad (3.4)$$

When measuring the ADC count distribution, it is important to insure that the primary charge is collected on one pad only. This is not always the case as in typical operating conditions a particle crossing the gap activates on average 1.1 pads [11]. A way to minimize this effect is to consider only events with a single hit. The ADC count distribution measured on one pad using such events is shown in Figure 2 (a). It exhibits an expected Landau shape with a peak around 120 ADC counts. At high counts a second peak is observed due to saturation of the preamplifier.

The Landau function most probable value m is adjusted on the measured distribution. The error on m depends on the number of events (between 200–500 depending on the pad position) and

(a)   (b)
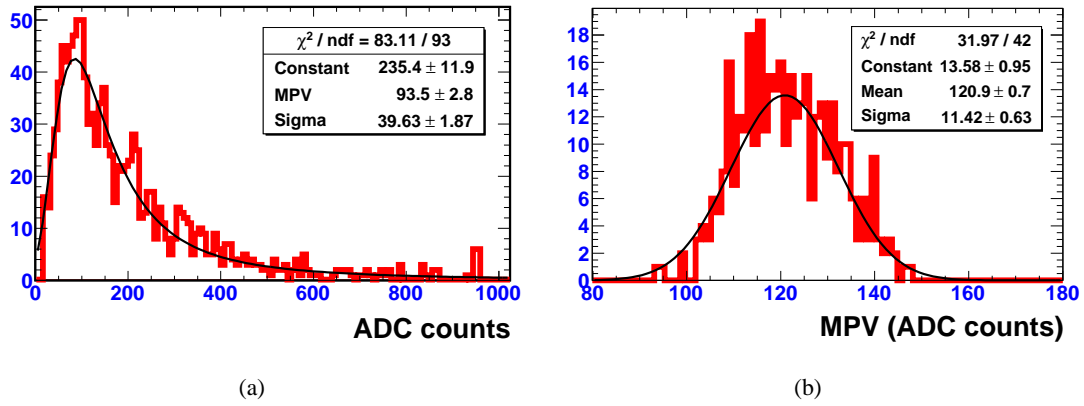
Figure 2. ADC count distribution measured on one pad (a). Most probable value of the adjusted Landau function for all pads (b).

was estimated by a Monte Carlo simulation. On most of the pads it is equal to 7 ADC counts. The Landau MPV averaged over all pads $\overline{m}$ is equal to 121 ADC counts with an r.m.s. of 12 counts (Figure 2 (b)). This corresponds to a most probable charge of 24 fC with variations of 12 %. Eventually, the number of ADC counts measured on a pad is multiplied by the correction factor:

$$a_i = \begin{cases} 1 - \mid 1 - w_i \mid & \text{for } w_i \geq 1 \\ 1 + \mid 1 - w_i \mid & \text{for } w_i < 1 \end{cases} \tag{3.5}$$

3.3 Pressure and temperature corrections

Pressure and temperature impact on the gas number density and hence on the ionisation mean free path. Eventually P and T variations result in a change of primary ionisation and gas gain. In our experimental conditions, the first can be safely neglected and only gas gain variations are considered. The gain dependence on P and T can be inferred from a simple model. Using the Rose and Korff parametrization of the Townsend coefficient α [12], the gain can be written as:

$$G = \exp(\alpha g) = \exp\left(\frac{APg}{T}\exp(-\frac{BPg}{TV})\right) \tag{3.6}$$

where A and B are constants that depend on the gas mixture, g is the amplification gap and V the mesh voltage. It follows that the gain relative sensitivity to P/T variations is given by:

$$C_{P/T} = \frac{1}{G}\frac{\partial G}{\partial (P/T)} = Ag\left(1 - \frac{Bg}{V}\frac{P}{T}\right)\exp\left(-\frac{Bg}{V}\frac{P}{T}\right) \tag{3.7}$$

The constants A and B are adjusted on the measured $G(V)$ trend, fixing P, T, g and V. In typical operating conditions, one obtains $C_{P/T}$ = -2.39 K/mbar in Ar/iC$_4$H$_{10}$ 95/5. A direct measurement of $C_{P/T}$ is detailed in [11]. The time variations of the P/T ratio during the beam test are shown in Figure 3 (a). Over the full test period, the average P and T are equal to 970 mbar and 298 K with variations of 20 mbar and 5 K r.m.s.. The measured number of ADC counts is multiplied by the correction factor a_t calculated as:

$$a_t = 1 - C_{P/T}\Delta(P/T) = 1 - C_{P/T}\left(\frac{P(t)}{T(t)} - \frac{P_0}{T_0}\right) \tag{3.8}$$

with P_0, T_0 the average values quoted above. The distribution of the correction factor a_t is shown in Figure 3 (b). The correction factor assumes a value between 0.80 and 1.15 with a dispersion of 8 % r.m.s..


(a)   (b)
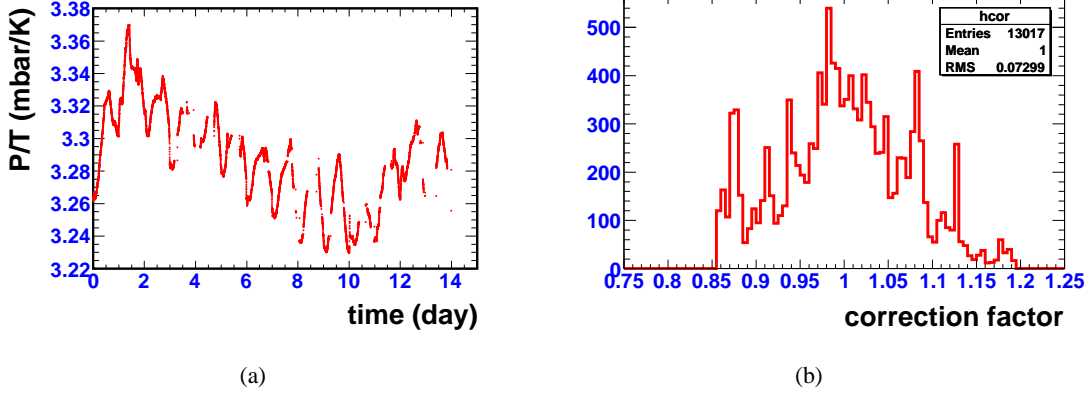
Figure 3. Pressure and temperature variations during the beam test (a). Correction factor applied to the measured number of ADC counts (b).

3.4 Longitudinal shower profile

The acquisition is triggered by the coincidence of the S_4 and S_5 signals in order to record tracks traversing the center of the chamber G_4. In addition the Čerenkov counter signal is used to select electrons or positrons. For a given number of absorber plates, roughly $40 \cdot 10^3$ events were recorded. To reject events with noise hits in G_4, at least one hit is requested in two of the three chambers (G_1–G_3). Moreover, in each chamber with at least one hit, the hit (or the hit with the largest number of ADC counts) should be centered at plus or minus one pad from the maximum of the beam profile. This insures that a track has traversed G_4 while reducing slightly the statistics ($30 \cdot 10^4$ events).

Energy distributions as measured with various number of absorbers are plotted in Figure 4 (a). The distributions of the number of hits are also shown (Figure 4 (b)). The longitudinal energy (resp. hit) profile is then obtained from the mean energy (resp. number of hits) deposited after each number of absorbers (Figure 5). The energy and number of hit profile are very similar, showing a maximum between 2 and 3 absorbers. The hit profile maximum, however, is reached at a slightly later stage of the shower development because at the beginning of the shower some secondary particles traverse the same pad.

A GEANT4 simulation of the beam test setup is being implemented. At the moment of writing, a threshold equal to 30 % of the most probable energy deposit is applied, the digitization of the energy is not performed and electronics saturation is neglected. The implementation of these effects in the simulation will be part of future work. The simulation predicts that the deposited energy is maximum after three absorbers. Considering the simplifying assumptions, this is in good agreement with our measurement. For more details on the simulation of the performance of a MICROMEGAS DHCAL, the reader is referred to [14].
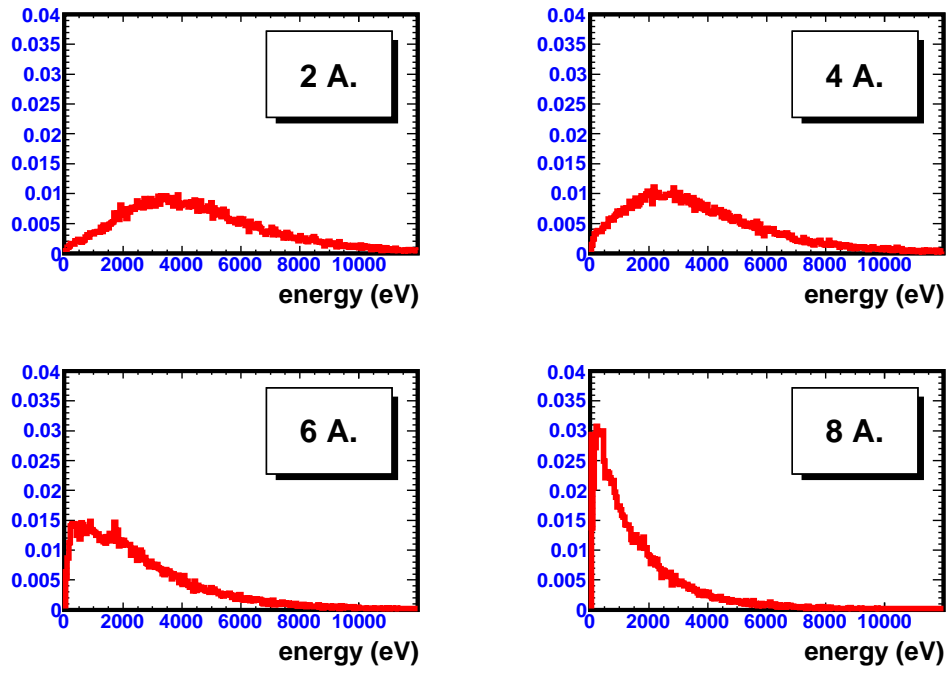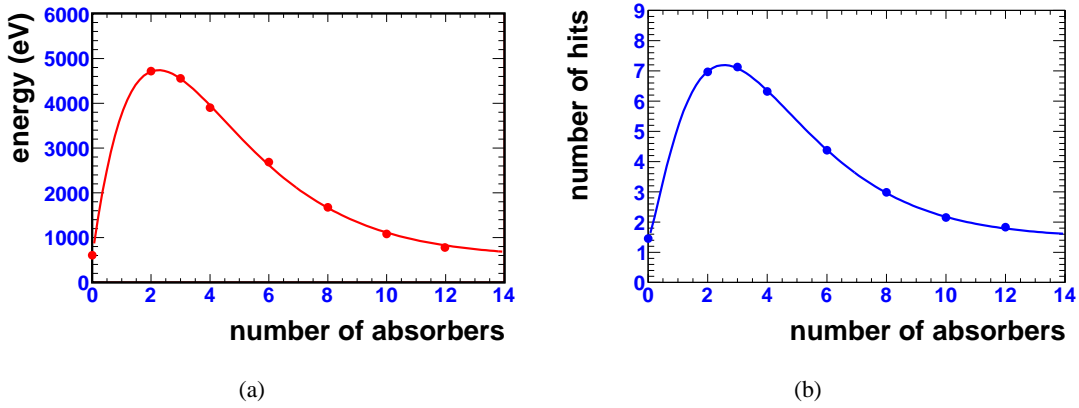
(a)
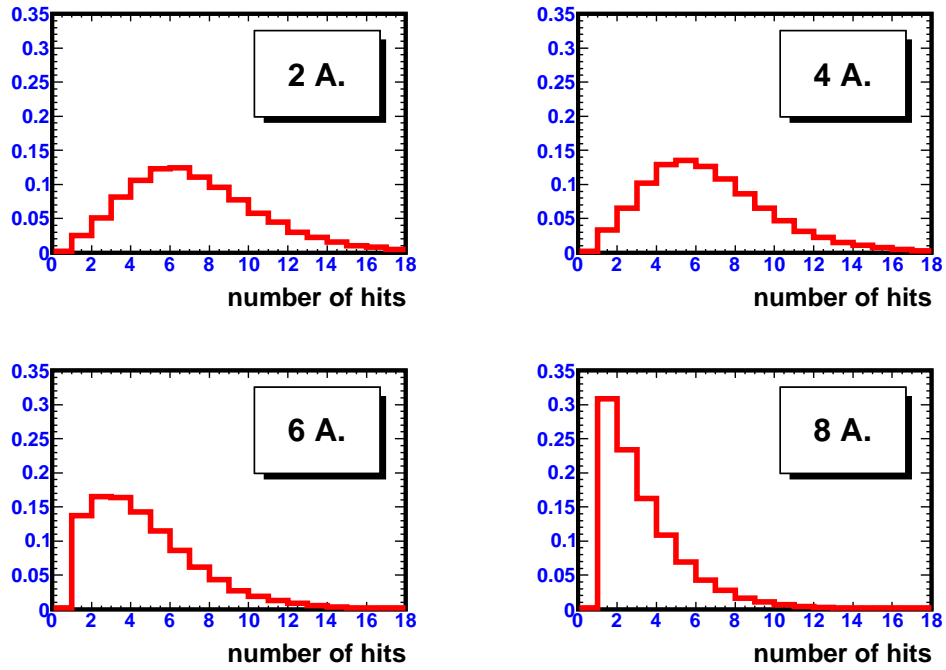
(b)

Figure 4. Energy (a) and number of hit (b) distributions from 2 GeV electron showers with various number of absorber plates. The distributions are normalized to one.

Figure 5. Mean energy (a) and number of hits (b) from 2 GeV electron showers as a function of the number of absorber plates.

3.5 Transverse shower profile

The transverse energy profile is the radial distribution of the energy in the chamber plane. The radial distance should be calculated as the distance between the intersection of the shower initiating particle track with the chamber plane (x_0, y_0) and the center of the hit pad. The coordinates (x_0, y_0), however, vary from one particle to the other. To minimize the spread, only tracks passing through the same single pads in the three small chambers G_1–G_3 are considered. These pads are determined as the maximum of the beam profile in each small chamber. The coordinates (x_0, y_0) are then taken as the center of the pad corresponding to the maximum of the beam profile in chamber G_4 when no absorber is present. Depending on the number of absorbers, between $1 \cdot 10^3$–$5 \cdot 10^3$ events are used.

The energy and hit radial distributions from 2 GeV electron/positron showers after various number of absorbers are shown in Figure 6 (a) and (b). Their shapes are similar, however, the energy distribution is slightly more peaked at the beginning of the shower (*e.g.* with two absorbers). This effect is illustrated in Figure 7 where the distribution r.m.s. is plotted as a function of the number of absorbers.

The profile of the number of hits exhibits a slightly larger r.m.s. than the energy profile. This can be explained by the fact that at the beginning of the shower development, a high number of secondary particles are crossing the same pad, thus inducing a high signal on the very central pads. When a threshold is applied on the energy, however, only one hit is counted no matter the number of particles crossing the central pads, leading to a less peaked distribution of the signal. At the maximum of the longitudinal profile (2–3 absorbers), the transverse profile r.m.s. is about 1.6–1.8 pads.

3.6 Conclusion

Shower profiles from 2 GeV electrons were measured with a 12×32 cm^2 MICROMEGAS chamber equipped with 1 cm^2 pads and GASSIPLEX chips. The detector was operated during 12 days in a beam of electrons, positrons and hadrons. At a gas gain of $17 \cdot 10^3$, the spark rate was very low (a few sparks per day) and no damage on the detector was observed. Although it was not stated, a detection efficiency of 97 % was previously measured at such a gas gain [11]. The energy and
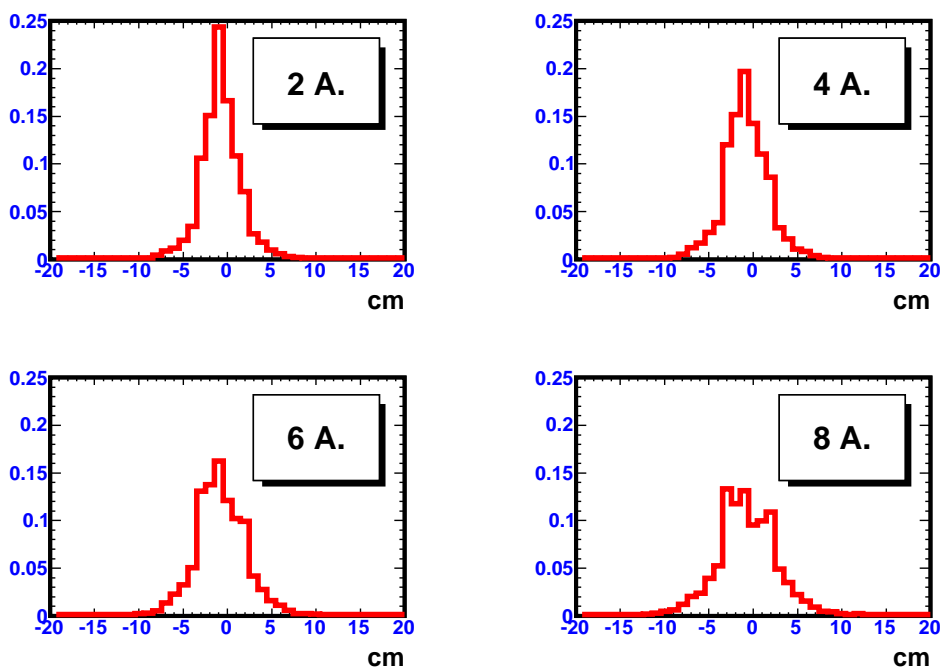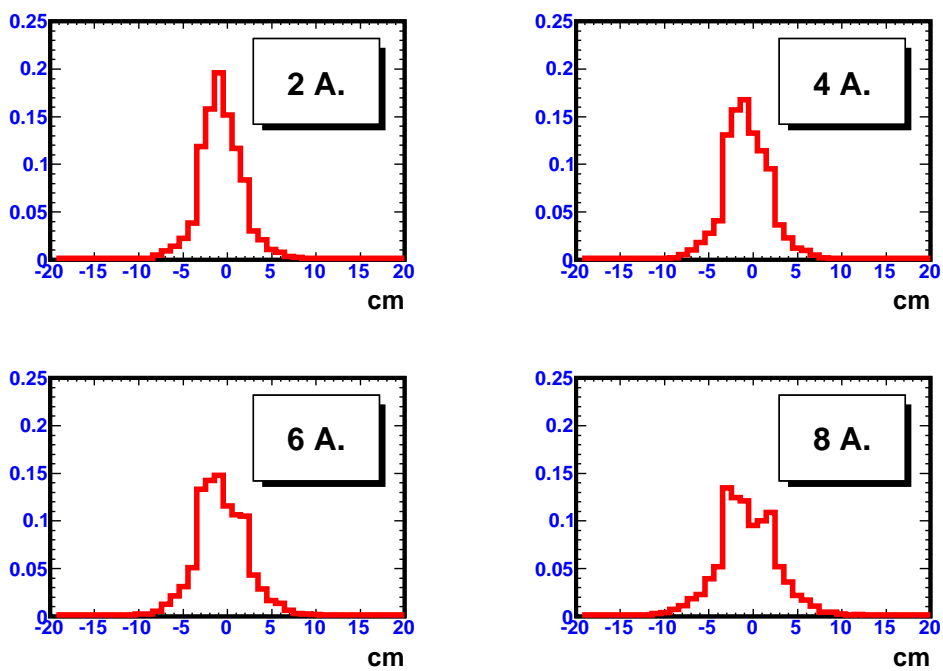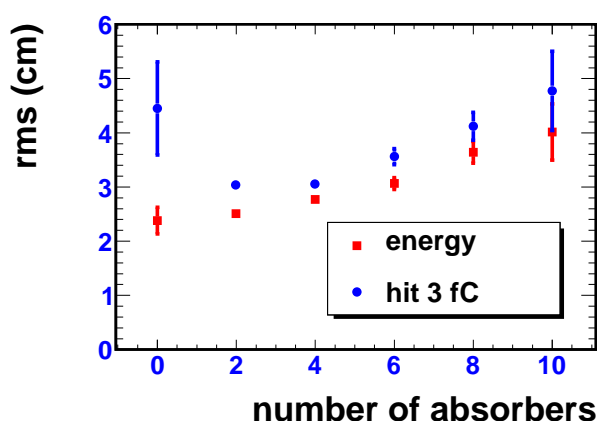
Figure 6. Energy (a) and number of hit (b) radial distributions from 2 GeV electron showers after various number of absorber plates.

Figure 7. R.m.s. of the radial distribution of the energy and the number of hits from 2 GeV electron showers.

number of hit profile are very similar. The longitudinal profile shows a maximum between 2 and 3 absorbers. In this configuration the transverse spread of the shower is about 1.6–1.8 pads r.m.s..

## 4. Chambers with embedded electronics

4.1 ASICs for digital calorimetry at ILC

The time structure of the electron and positron beams at ILC would consist of 1 ms long bunch trains with a bunch crossing period of 300 ns, separated by 199 ms. During this idle time, it is proposed to switch off the front-end electronics of the detectors. Based on this power pulsing scheme, the HARDROC and DIRAC ASICs were designed to meet the requirements of a digital hadronic calorimeter. They are 64 channel self-triggered integrated circuits, each channel being equipped with an adjustable gain preamplifier, two (three for DIRAC) comparators and a memory. Each channel mainly provides a digital information.

An essential point of HARDROC and DIRAC-based chambers is that they can be made very thin. Thanks to the Bulk fabrication process, anode PCBs with chips connected on the backside can be equipped with a mesh. The overall thickness remains below 8 mm including the chamber cover which will be part of the absorber. This already complies with ILC constraints on the DHCAL gap size between absorbers. Moreover, the Bulk is used by several experiments with large areas to instrument [13, 15]. It is thus well suited for the construction of a 1 m^3 DHCAL MICROMEGAS prototype.

4.2 First chamber tests and future plans

Chambers with one DIRAC (8×8 cm^2) or four HARDROCs (8×32 cm^2) have been constructed (Figure 8 (a) and (b)). They are dubbed ASU: Active Sensor Unit. The DIRAC chamber was placed in a 200 GeV pion beam in August 2008 at the SPS (Figure 9 (a)). A stack of four chambers should be available in October 2009. It will be used for measuring efficiency and hit multiplicity at the CERN/PS. For recent measurements of the characteristics of DIRAC, the reader is referred to [16].
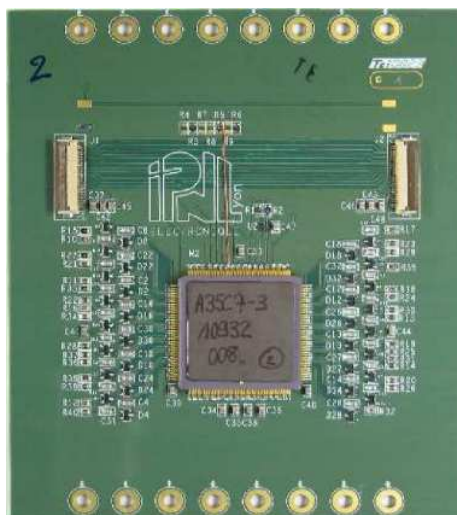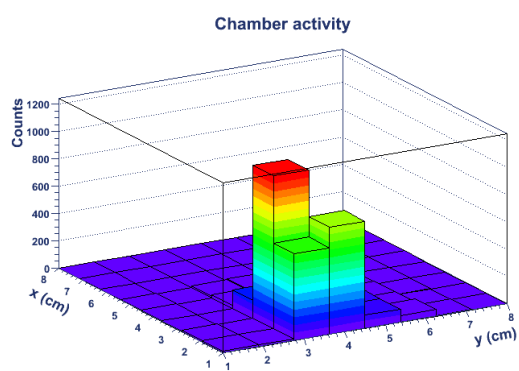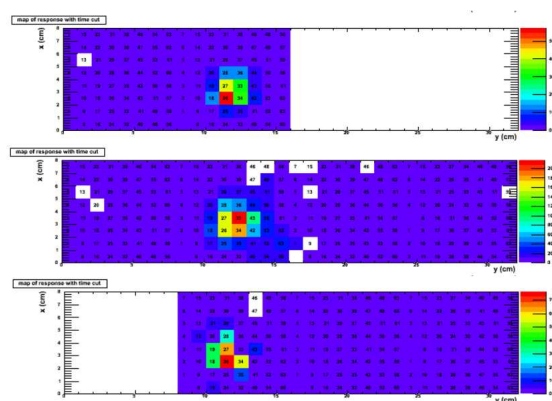
(a)
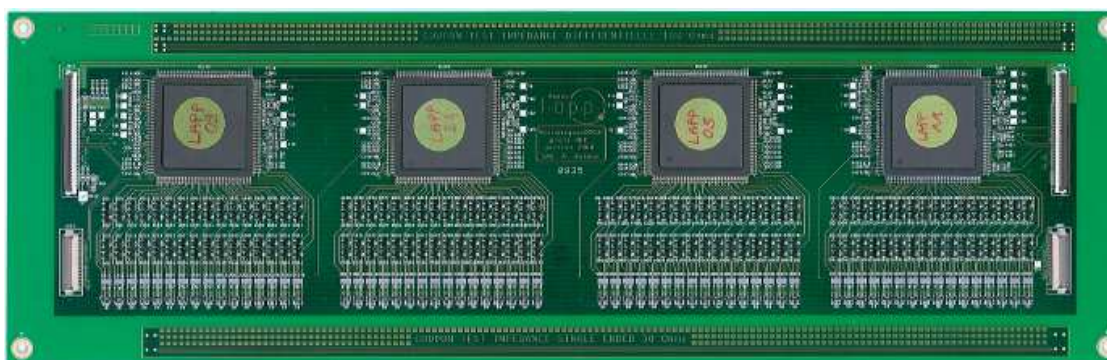
(b)

Figure 8. Photograph of the PCB backside of DIRAC (a) and HARDROC (b) based chambers.

(a)

(b)

Figure 9. Beam profile measured with one DIRAC (a) and three HARDROC (b) chambers. The hotter the color the larger the number of hits recorded on a given pad. Each pad has an area of 1 cm^2.

Three ASUs with four HARDROCs were placed in a 2 GeV electron beam at the CERN/PS. Despite dead zones due to faulty chips, a clear image of the beam profile in the anode plane is obtained in each chamber (Figure 9 (b)). In view of the construction of a 1 m^3 MICROMEGAS DHCAL made of 40 planes, a 1 m^2 chamber is being assembled. It consists of six 32×48 cm^2 ASUs brought together in a single gas volume. Each ASU is equipped with 24 HARDROC (version 2) chips (Figure 10). Measurements of the performance of HARDROC based chambers are foreseen in the October 2009 at the CERN/PS.

Figure 10. Photograph of two PCBs equipped with 24 HARDROCs each. The active area of a PCB is 32×48 cm^2.

5. Conclusion

Bulk MICROMEGAS chambers equipped with GASSIPLEX chips were used to measure the spatial characteristics of 2 GeV electron showers at the CERN/PS. During twelve days, the chambers were operated at high gas gain ($17 \cdot 10^3$) in Ar/iC$_4$H$_{10}$ 95/5 while the spark rate was negligibly low. Longitudinal and transverse profile of the energy and number of hits were measured. These results will soon be confronted to GEANT4 predictions. This will constitute a good test of the simulation.

In view of the construction of a MICROMEGAS DHCAL, 8 mm thin chambers with digital readout embedded on the backside of the anode PCB were fabricated. The first test was carried out in 2008 with an 8×8 cm^2 chambers equipped with a DIRAC chip at the CERN/SPS facility. In 2009, 8×32 cm^2 chambers equipped with HARDROCs were tested in the CERN/PS beam. Signals from the beam particles were recorded, demonstrating the feasibility of thin MICROMEGAS chambers. The next step is to build and test larger area chambers. For that purpose, two 32×48 cm^2 PCBs were recently equipped with twenty four HARDROCs (version 2) each and a mesh. Tests of the electronics and of their amplification properties will be carried out at LAPP in the coming months. Eventually they should be tested in a beam at the end of the year 2009 inside a 1 m^2 chamber.

Nicolas Geffroy and Fabrice Peltier for their decisive contribution to the assembly of the chambers and the installation of the beam test setup. Thanks also to L. Fournier and J. Jacquemier for their creative work on the reconstruction/analysis software.

References

[1] ILC Reference Design Report, Detectors (2007).

[2] F. Sauli, *Nucl. Instr. and Meth. A* **386** (1997) 531.

[3] J. Yu, GEM DHCal Development, *Proceedings of the Linear Collider Workshop* DESY, Hamburg (2007).

[4] B. Bilki *et al.*, *JINST* P04006 **4** (2009).

[5] I. Giomataris *et al.*, *Nucl. Instr. and Meth. A* **376** (1996) 29.

[6] C. Adloff *et al.*, Development of MICROMEGAS for a Digital Hadronic Calorimeter, *Proceedings of the Linear Collider Workshop*, Chicago (2008).

[7] GASSIPLEX, A 16 integrated channels front-end analog amplifiers with multiplexed serial readout, Ref. PC 2000/107 (2000), http://www-subatech.in2p3.fr.

[8] V. Boudry *et al.*, HARDROC1, Readout chip of the Digital Hadronic Calorimeter of ILC, *IEEE-NSS conference records* (2007).

[9] R. Gaglione and H. Mathez, DIRAC: a Digital Readout Asic for hAdronic Calorimeter, *IEEE-NSS conference records* **1** (2008) 1815.

[10] S. Andriamonje *et al.*, *Nucl. Instr. and Meth. A* **560** (2006) 405.

[11] C. Adloff *et al.*, MICROMEGAS chambers for hadronic calorimetry at a future linear collider, to be submitted to JINST.

[12] F. Sauli, Principles of operation of Multiwire Proportional and Drift Chambers, CERN Yellow Reports 77-09 (1977).

[13] T. Alexopoulos *et al.*, *Nucl. Instr. and Meth. A* (2009), doi:10.1016/j.nima.2009.06.113.

[14] C. Adloff *et al.*, Monte carlo study of the physics performance of a digital hadronic calorimeter, *Proceedings of the MPGD Conference*, Kolymbari (2009).

[15] S. Anvar *et al.*, *Nucl. Instr. and Meth. A* **602** (2009) 415.

[16] C. Adloff *et al.*, MICROMEGAS chamber with embedded DIRAC ASIC for hadronic calorimetry, *Proceedings of the MPGD Conference*, Kolymbari (2009).